

# Reaction-rate measurements of cold ion-polar molecule reactions with a combined Stark-velocity-filter—ion-trap apparatus

B1278373 Masanari Ichikawa  
Atomic Physics Laboratory

## 1. Introduction

There is a space where gas and molecules are gathering, making chemical reactions and forming stars in the universe-known as an interstellar molecular cloud. It is necessary to understand chemical evolution of molecular clouds for understanding how stars are formed [1, 2]. The time-evolution of their chemical compositions are numerically calculated by applying various reaction networks based on reaction databases, such as UMIST database [3]. However, most of the measurements of ion-neutral reactions were only at room temperature or at a restricted range of temperatures near room temperature, even though the reactions occur at low temperatures in interstellar clouds. Almost of the reaction-rate constants compiled in databases were measured by conventional swarm techniques, such as selected ion-flow tube and flowing afterglow, under high pressure conditions [4]. Especially for cold ion-polar molecule reactions extensive laboratory studies have not been performed because it is hard to supply cold polar molecules in gas phase owing to condensation of polar gases at low temperatures.

For that reason, we have developed a combined Stark-velocity-filter-ion-trap apparatus for the purpose of reaction-rate measurements between cold molecular ions and slow polar molecules under ultra-high vacuum conditions [5, 6].

In this work, we investigated cold ion-polar molecule reactions between sympathetically cooled  $\text{N}_2\text{H}^+$  and slow polar molecules, namely  $\text{CD}_3\text{CN}$  and  $\text{CH}_3\text{OH}$ . The reaction-rate constants, which were measured at lower than 10 K, were compared to theoretical values by the scaling formula [7] in addition to the locked dipole approximation. The reaction energy diagrams of these reaction-systems were determined to discuss the reaction paths.

## 2. Experimental Setup

Figure 1 shows the reaction vacuum chamber containing a cryogenic linear Paul trap, an electron gun and the end section of the Stark velocity filter. The linear Paul trap consists of four segmented stainless steel rods with a diameter of 8 mm and the inner radius is 3.5 mm. The driving frequency and the amplitude of the trap are typically 4.56 MHz and 194 V, respectively. The ion trap is cooled by liquid nitrogen baffle to minimize background molecules.

Thus, the ultrahigh vacuum condition ( $< 3 \times 10^{-8}$  Pa) is maintained during reaction-rate measurements. The coolant  $\text{Ca}^+$  ions are produced and trapped by the laser ablation method, in which Nd:YAG pulsed laser is irradiated to a calcium bulk. The molecular ions are produced by electron-impact ionization using the electron gun, where the electron energy is typically 250 eV.

For laser cooling of  $\text{Ca}^+$  ions, two diode lasers with oscillation wavelengths of 397 and 866 nm are used. As shown in Fig.1, the laser beams pass through the trap center along the trap axis. The laser induced fluorescence (LIF) from  $\text{Ca}^+$  ions is detected by a cooled CCD camera as well as a photomultiplier tube (PMT) from the top of the photograph. The LIF image of  $\text{Ca}^+$  Coulomb crystal is focused on the CCD image sensor by a telecentric lens system with a magnification of  $\times 10$  or  $\times 6$ .

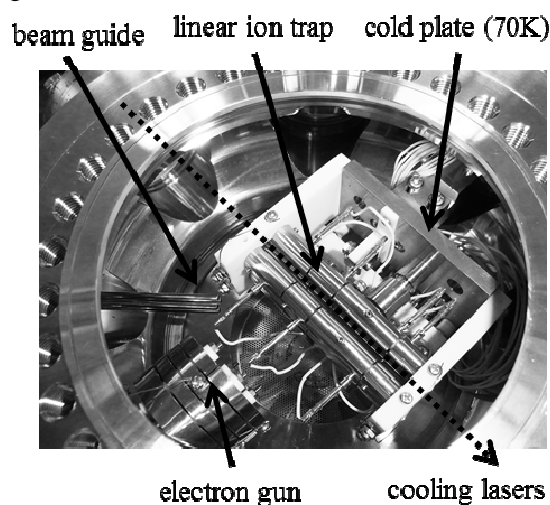


Fig1. A photograph of the reaction vacuum chamber.

## 3. Experimental Procedure

The measurement procedure is as follows. First, we produce a  $\text{Ca}^+$  Coulomb crystal in the linear Paul trap. Then a nitrogen molecular gas of about  $1 \times 10^{-7}$  Pa is leaked into the vacuum chamber using a variable leak valve and the electron beam is incident to the center of the ion trap where  $\text{N}_2^+$  molecular ions are produced by electron impact ionization. The produced  $\text{N}_2^+$  ions are sympathetically cooled and gathering around the trap axis. After the preparation of cold  $\text{N}_2^+$  ions, a hydrogen molecular gas of about  $6 \times 10^{-6}$  Pa is introduced into the vacuum chamber. All of  $\text{N}_2^+$  ions

change into  $N_2H^+$  by the reactions of  $N_2^+ + H_2 \rightarrow N_2H^+ + H$  during the reaction time of 240 s [8]. As shown in the left in Fig. 3, the produced  $N_2H^+$  ions are trapped in the center dark area and are sympathetically cooled to sub-Kelvin temperature by laser-cooled  $Ca^+$  ions. Then slow polar molecules generated by the Stark velocity filter are irradiated to the two species Coulomb crystal containing  $Ca^+$  and  $N_2H^+$ . The reaction rate is measured by observing a change of a fluorescence image of a  $Ca^+$  Coulomb crystal. Actually we determine the relative number of molecular ions from the volume of the dark area in the observed fluorescence images under the assumption of the constant number density and the cylindrical symmetry of the spatial distribution of cold  $N_2H^+$  ions.

In order to check the validity of this method, we performed molecular dynamics (MD) simulations of two-species Coulomb crystals containing thousands of ions by newly developing accelerated calculation system (GRAPE9). A good correlation between the volumes estimated from the simulation images and the number of  $N_2H^+$  ions was obtained as long as there are sufficient number of molecular ions so that the ions extend to both ends of the  $Ca^+$  Coulomb crystal (see figure 2). This method facilitates the image data analysis and frees us from troublesome MD simulations.

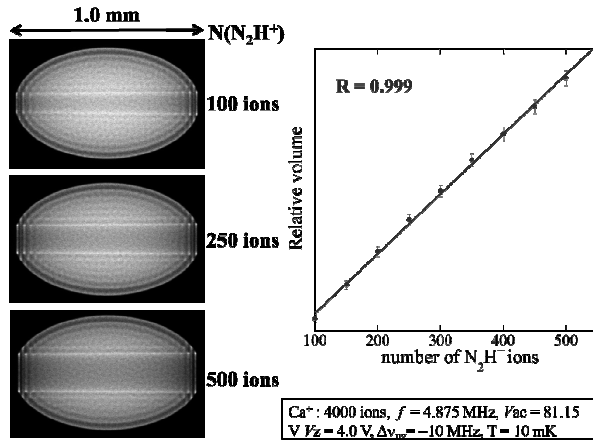


Fig.2 Simulation images of two-species Coulomb crystal containing 4000  $Ca^+$  and several hundreds of  $N_2H^+$  ions. The assumed secular temperature of the  $Ca^+$  ions is 10 mK. The correlation coefficient of the estimated volumes of the dark areas and the numbers of  $N_2H^+$  is about  $R = 0.999$ .

#### 4. Result and Discussion

Figure 3 shows the snap shots of the LIF images of the two-species Coulomb crystal during irradiating slow  $CD_3CN$  molecules. The dark area containing  $N_2H^+$  progressively decreases with increasing reaction time. Figure 4 shows the decay curve of the relative number of  $N_2H^+$  as a function of the reaction time. In this example, the reaction rate is determined to be  $1.2(5) \times 10^{-3} s^{-1}$ . We performed 7 measurements and

averaged the reaction rates to determine the reaction-rate constant. Using the number density of the velocity-selected  $CD_3CN$ , which was separately determined, the reaction-rate constant is also determined to be  $k = 1.0(3) \times 10^{-8} cm^3 s^{-1}$ . It is noted that the average reaction energy is estimated to be about 3 K in the present experimental conditions. The main contribution to the error is considered to be the uncertainty of the number density of  $CD_3CN$ .

The present reaction-rate constant is consistent with the estimated capture rate,  $k_{ts} = 3.79 \times 10^{-8} cm^3 s^{-1}$  calculated by the scaling formula [7], which is considered to be the maximum value of the reaction-rate constant. We also performed the same measurements for slow  $CH_3OH$  and  $CH_3CN$ . It is considered that the scaling formula overestimate the reaction-rate constants of these reactions by a factor of 2~3 compared to the experimental results. The results and discussions will be reported in detail at the oral presentation.

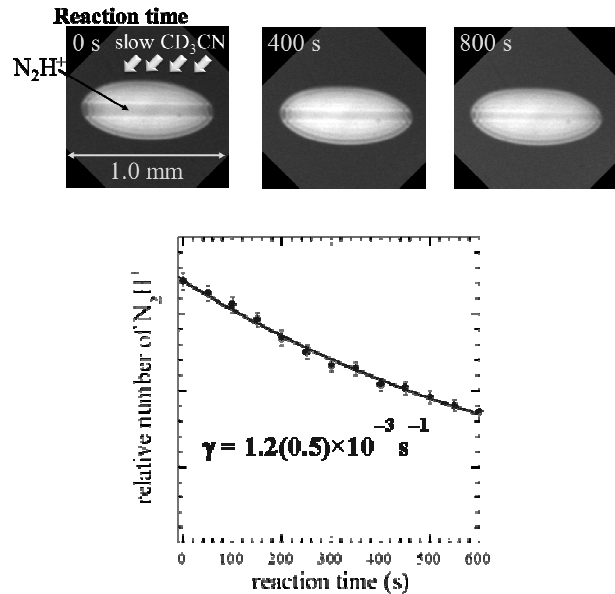


Fig.3 (a) Sequential LIF images of the two-species Coulomb crystal containing  $Ca^+$  and  $N_2H^+$  during  $CD_3CN + N_2H^+ \rightarrow CD_3CNH^+ + N_2$  reactions. (b) A plot of the relative number of  $N_2H^+$  ions estimated from the results of Fig.3 as a function of the reaction time.

#### Reference

- [1] E. Herbst and W. Klempler, *ApJ* **185**, 505 (1973).
- [2] V. Wakelam *et al.*, *Space Sci. Rev.* **156**, 13 (2010).
- [3] D. McElroy *et al.*, *Astronomy & Astrophysics* **550**, 36(2013).
- [4] N.G. Adams, D. Smith, *Int. J Mass Spectrom. Ion Phys.* **21**, 349 (1976).
- [5] T. Furukawa, *Master Thesis*, Sophia University (2013).
- [6] K. Okada *et al.*, *PRA* **87**, 043427 (2013).
- [7] T. Su *et al.*, *JCP* **76**, 5183 (1982).
- [8] D. Smith *et al.*, *JCP* **69**, 308 (1978).